

A Measurement of the Neutral B Meson Lifetime using Partially Reconstructed $B^0 \rightarrow D^{*-} \pi^+$ Decays

The *BABAR* Collaboration

November 3, 2018

Abstract

The neutral B meson lifetime has been measured with the data collected by the *BABAR* detector at the PEP-II storage ring during the year 2000 for a total integrated luminosity of 20.3 fb^{-1} . The $B^0 \rightarrow D^{*-} \pi^+$ decays have been selected with a partial reconstruction method in which only the fast pion from the B^0 decay and the slow pion from $D^{*-} \rightarrow \bar{D}^0 \pi^-$ are reconstructed. The B^0 lifetime has been measured to be $1.510 \pm 0.040 \pm 0.038 \text{ ps}$ with a sample of 6971 ± 241 reconstructed signal events.

Submitted to the XXXVIIth Rencontres de Moriond on QCD and Hadronic Interactions,
3/16/2002—3/23/2002, Les Arcs, France

Stanford Linear Accelerator Center, Stanford University, Stanford, CA 94309

Work supported in part by Department of Energy contract DE-AC03-76SF00515.

The BABAR Collaboration,

B. Aubert, D. Boutigny, J.-M. Gaillard, A. Hicheur, Y. Karyotakis, J. P. Lees, P. Robbe, V. Tisserand,
A. Zghiche

Laboratoire de Physique des Particules, F-74941 Annecy-le-Vieux, France

A. Palano, A. Pompili

Università di Bari, Dipartimento di Fisica and INFN, I-70126 Bari, Italy

G. P. Chen, J. C. Chen, N. D. Qi, G. Rong, P. Wang, Y. S. Zhu

Institute of High Energy Physics, Beijing 100039, China

G. Eigen, I. Ofte, B. Stugu

University of Bergen, Inst. of Physics, N-5007 Bergen, Norway

G. S. Abrams, A. W. Borgland, A. B. Breon, D. N. Brown, J. Button-Shafer, R. N. Cahn, E. Charles,
M. S. Gill, A. V. Gritsan, Y. Groysman, R. G. Jacobsen, R. W. Kadel, J. Kadyk, L. T. Kerth,
Yu. G. Kolomensky, J. F. Kral, C. LeClerc, M. E. Levi, G. Lynch, L. M. Mir, P. J. Oddone, M. Pripstein,
N. A. Roe, A. Romosan, M. T. Ronan, V. G. Shelkov, A. V. Telnov, W. A. Wenzel

Lawrence Berkeley National Laboratory and University of California, Berkeley, CA 94720, USA

T. J. Harrison, C. M. Hawkes, D. J. Knowles, S. W. O'Neale, R. C. Penny, A. T. Watson, N. K. Watson

University of Birmingham, Birmingham, B15 2TT, United Kingdom

T. Deppermann, K. Goetzen, H. Koch, B. Lewandowski, K. Peters, H. Schmuecker, M. Steinke

Ruhr Universität Bochum, Institut für Experimentalphysik 1, D-44780 Bochum, Germany

N. R. Barlow, W. Bhimji, N. Chevalier, P. J. Clark, W. N. Cottingham, B. Foster, C. Mackay, F. F. Wilson

University of Bristol, Bristol BS8 1TL, United Kingdom

K. Abe, C. Hearty, T. S. Mattison, J. A. McKenna, D. Thiessen

University of British Columbia, Vancouver, BC, Canada V6T 1Z1

S. Jolly, A. K. McKemey

Brunel University, Uxbridge, Middlesex UB8 3PH, United Kingdom

V. E. Blinov, A. D. Bukin, D. A. Bukin, A. R. Buzykaev, V. B. Golubev, V. N. Ivanchenko, A. A. Korol,
E. A. Kravchenko, A. P. Onuchin, S. I. Serednyakov, Yu. I. Skovpen, A. N. Yushkov

Budker Institute of Nuclear Physics, Novosibirsk 630090, Russia

D. Best, M. Chao, D. Kirkby, A. J. Lankford, M. Mandelkern, S. McMahon, D. P. Stoker

University of California at Irvine, Irvine, CA 92697, USA

K. Arisaka, C. Buchanan, S. Chun

University of California at Los Angeles, Los Angeles, CA 90024, USA

D. B. MacFarlane, S. Prell, Sh. Rahatlou, G. Raven, V. Sharma

University of California at San Diego, La Jolla, CA 92093, USA

C. Campagnari, B. Dahmes, P. A. Hart, N. Kuznetsova, S. L. Levy, O. Long, A. Lu, M. A. Mazur,
J. D. Richman, W. Verkerke

University of California at Santa Barbara, Santa Barbara, CA 93106, USA

J. Beringer, A. M. Eisner, M. Grothe, C. A. Heusch, W. S. Lockman, T. Pulliam, T. Schalk, R. E. Schmitz,
B. A. Schumm, A. Seiden, M. Turri, W. Walkowiak, D. C. Williams, M. G. Wilson

University of California at Santa Cruz, Institute for Particle Physics, Santa Cruz, CA 95064, USA

E. Chen, G. P. Dubois-Felsmann, A. Dvoretzskii, D. G. Hitlin, S. Metzler, J. Oyang, F. C. Porter, A. Ryd,
A. Samuel, S. Yang, R. Y. Zhu

California Institute of Technology, Pasadena, CA 91125, USA

S. Jayatilke, G. Mancinelli, B. T. Meadows, M. D. Sokoloff

University of Cincinnati, Cincinnati, OH 45221, USA

T. Barillari, P. Bloom, W. T. Ford, U. Nauenberg, A. Olivas, P. Rankin, J. Roy, J. G. Smith, W. C. van
Hoek, L. Zhang

University of Colorado, Boulder, CO 80309, USA

J. Blouw, J. L. Harton, M. Krishnamurthy, A. Soffer, W. H. Toki, R. J. Wilson, J. Zhang

Colorado State University, Fort Collins, CO 80523, USA

T. Brandt, J. Brose, T. Colberg, M. Dickopp, R. S. Dubitzky, A. Hauke, E. Maly, R. Müller-Pfefferkorn,
S. Otto, K. R. Schubert, R. Schwierz, B. Spaan, L. Wilden

Technische Universität Dresden, Institut für Kern- und Teilchenphysik, D-01062 Dresden, Germany

D. Bernard, G. R. Bonneaud, F. Brochard, J. Cohen-Tanugi, S. Ferrag, S. T'Jampens, Ch. Thiebaux,
G. Vasileiadis, M. Verderi

Ecole Polytechnique, LLR, F-91128 Palaiseau, France

A. Anjomshoaa, R. Bernet, A. Khan, D. Lavin, F. Muheim, S. Playfer, J. E. Swain, J. Tinslay

University of Edinburgh, Edinburgh EH9 3JZ, United Kingdom

M. Falbo

Elon University, Elon College, NC 27244-2010, USA

C. Borean, C. Bozzi, L. Piemontese

Università di Ferrara, Dipartimento di Fisica and INFN, I-44100 Ferrara, Italy

E. Treadwell

Florida A&M University, Tallahassee, FL 32307, USA

F. Anulli,¹ R. Baldini-Ferrolì, A. Calcaterra, R. de Sangro, D. Falciari, G. Finocchiaro, P. Patteri,
I. M. Peruzzi,² M. Piccolo, Y. Xie, A. Zallo

Laboratori Nazionali di Frascati dell'INFN, I-00044 Frascati, Italy

S. Bagnasco, A. Buzzo, R. Contri, G. Crosetti, M. Lo Vetere, M. Macri, M. R. Monge, S. Passaggio,
F. C. Pastore, C. Patrignani, E. Robutti, A. Santroni, S. Tosi

Università di Genova, Dipartimento di Fisica and INFN, I-16146 Genova, Italy

¹ Also with Università di Perugia, I-06100 Perugia, Italy

² Also with Università di Perugia, I-06100 Perugia, Italy

M. Morii

Harvard University, Cambridge, MA 02138, USA

R. Bartoldus, R. Hamilton, U. Mallik

University of Iowa, Iowa City, IA 52242, USA

J. Cochran, H. B. Crawley, J. Lamsa, W. T. Meyer, E. I. Rosenberg, J. Yi

Iowa State University, Ames, IA 50011-3160, USA

G. Grosdidier, A. Höcker, H. M. Lacker, S. Laplace, F. Le Diberder, V. Lepeltier, A. M. Lutz,
S. Plaszczynski, M. H. Schune, S. Trincaz-Duvoid, G. Wormser

Laboratoire de l'Accélérateur Linéaire, F-91898 Orsay, France

R. M. Bionta, V. Brigljević, D. J. Lange, M. Mugge, K. van Bibber, D. M. Wright

Lawrence Livermore National Laboratory, Livermore, CA 94550, USA

A. J. Bevan, J. R. Fry, E. Gabathuler, R. Gamet, M. George, M. Kay, D. J. Payne, R. J. Sloane,
C. Touramanis

University of Liverpool, Liverpool L69 3BX, United Kingdom

M. L. Aspinwall, D. A. Bowerman, P. D. Dauncey, U. Egede, I. Eschrich, G. W. Morton, J. A. Nash,
P. Sanders, D. Smith

University of London, Imperial College, London, SW7 2BW, United Kingdom

J. J. Back, G. Bellodi, P. Dixon, P. F. Harrison, R. J. L. Potter, H. W. Shorthouse, P. Strother, P. B. Vidal

Queen Mary, University of London, E1 4NS, United Kingdom

G. Cowan, S. George, M. G. Green, A. Kurup, C. E. Marker, T. R. McMahon, S. Ricciardi, F. Salvatore,
G. Vaitsas

University of London, Royal Holloway and Bedford New College, Egham, Surrey TW20 0EX, United Kingdom

D. Brown, C. L. Davis

University of Louisville, Louisville, KY 40292, USA

J. Allison, R. J. Barlow, J. T. Boyd, A. C. Forti, F. Jackson, G. D. Lafferty, N. Savvas, J. H. Weatherall,
J. C. Williams

University of Manchester, Manchester M13 9PL, United Kingdom

A. Farbin, A. Jawahery, V. Lillard, J. Olsen, D. A. Roberts, J. R. Schieck

University of Maryland, College Park, MD 20742, USA

G. Blaylock, C. Dallapiccola, K. T. Flood, S. S. Hertzbach, R. Kofler, V. B. Koptchev, T. B. Moore,
H. Staengle, S. Willocq

University of Massachusetts, Amherst, MA 01003, USA

B. Brau, R. Cowan, G. Sciolla, F. Taylor, R. K. Yamamoto

Massachusetts Institute of Technology, Laboratory for Nuclear Science, Cambridge, MA 02139, USA

M. Milek, P. M. Patel

McGill University, Montréal, QC, Canada H3A 2T8

F. Palombo, C. Vite

Università di Milano, Dipartimento di Fisica and INFN, I-20133 Milano, Italy

J. M. Bauer, L. Cremaldi, V. Eschenburg, R. Kroeger, J. Reidy, D. A. Sanders, D. J. Summers

University of Mississippi, University, MS 38677, USA

C. Hast, J. Y. Nief, P. Taras

Université de Montréal, Laboratoire René J. A. Lévesque, Montréal, QC, Canada H3C 3J7

H. Nicholson

Mount Holyoke College, South Hadley, MA 01075, USA

C. Cartaro, N. Cavallo,³ G. De Nardo, F. Fabozzi, C. Gatto, L. Lista, P. Paolucci, D. Piccolo, C. Sciacca

Università di Napoli Federico II, Dipartimento di Scienze Fisiche and INFN, I-80126, Napoli, Italy

J. M. LoSecco

University of Notre Dame, Notre Dame, IN 46556, USA

J. R. G. Alsmiller, T. A. Gabriel

Oak Ridge National Laboratory, Oak Ridge, TN 37831, USA

J. Brau, R. Frey, E. Grauges, M. Iwasaki, C. T. Potter, N. B. Sinev, D. Strom

University of Oregon, Eugene, OR 97403, USA

F. Colecchia, F. Dal Corso, A. Dorigo, F. Galeazzi, M. Margoni, M. Morandin, M. Posocco, M. Rotondo,
F. Simonetto, R. Stroili, E. Torassa, C. Voci

Università di Padova, Dipartimento di Fisica and INFN, I-35131 Padova, Italy

M. Benayoun, H. Briand, J. Chauveau, P. David, Ch. de la Vaissière, L. Del Buono, O. Hamon,
Ph. Leruste, J. Ocariz, M. Pivk, L. Roos, J. Stark

Universités Paris VI et VII, Lab de Physique Nucléaire H. E., F-75252 Paris, France

P. F. Manfredi, V. Re, V. Speziali

Università di Pavia, Dipartimento di Elettronica and INFN, I-27100 Pavia, Italy

E. D. Frank, L. Gladney, Q. H. Guo, J. Panetta

University of Pennsylvania, Philadelphia, PA 19104, USA

C. Angelini, G. Batignani, S. Bettarini, M. Bondioli, F. Bucci, E. Campagna, M. Carpinelli, F. Forti,
M. A. Giorgi, A. Lusiani, G. Marchiori, F. Martinez-Vidal, M. Morganti, N. Neri, E. Paoloni, M. Rama,
G. Rizzo, F. Sandrelli, G. Simi, G. Triggiani, J. Walsh

Università di Pisa, Scuola Normale Superiore and INFN, I-56010 Pisa, Italy

M. Haire, D. Judd, K. Paick, L. Turnbull, D. E. Wagoner

Prairie View A&M University, Prairie View, TX 77446, USA

J. Albert, P. Elmer, C. Lu, V. Miftakov, S. F. Schaffner, A. J. S. Smith, A. Tumanov, E. W. Varnes

Princeton University, Princeton, NJ 08544, USA

³ Also with Università della Basilicata, I-85100 Potenza, Italy

F. Bellini, G. Cavoto, D. del Re, R. Faccini,⁴ F. Ferrarotto, F. Ferroni, M. A. Mazzoni, S. Morganti,
G. Piredda, M. Serra, C. Voena

Università di Roma La Sapienza, Dipartimento di Fisica and INFN, I-00185 Roma, Italy

S. Christ, R. Waldi

Universität Rostock, D-18051 Rostock, Germany

T. Adye, N. De Groot, B. Franek, N. I. Geddes, G. P. Gopal, S. M. Xella

Rutherford Appleton Laboratory, Chilton, Didcot, Oxon, OX11 0QX, United Kingdom

R. Aleksan, S. Emery, A. Gaidot, S. F. Ganzhur, P.-F. Giraud, G. Hamel de Monchenault, W. Kozanecki,
M. Langer, G. W. London, B. Mayer, B. Serfass, G. Vasseur, Ch. Yèche, M. Zito

DAPNIA, Commissariat à l'Energie Atomique/Saclay, F-91191 Gif-sur-Yvette, France

M. V. Purohit, A. W. Weidemann, F. X. Yumiceva

University of South Carolina, Columbia, SC 29208, USA

I. Adam, D. Aston, N. Berger, A. M. Boyarski, G. Calderini, M. R. Convery, D. P. Coupal, D. Dong,
J. Dorfan, W. Dunwoodie, R. C. Field, T. Glanzman, S. J. Gowdy, T. Haas, T. Hadig, V. Halyo, T. Himel,
T. Hryn'ova, M. E. Huffer, W. R. Innes, C. P. Jessop, M. H. Kelsey, P. Kim, M. L. Kocian,
U. Langenegger, D. W. G. S. Leith, S. Luitz, V. Luth, H. L. Lynch, H. Marsiske, S. Menke, R. Messner,
D. R. Muller, C. P. O'Grady, V. E. Ozcan, A. Perazzo, M. Perl, S. Petrak, H. Quinn, B. N. Ratcliff,
S. H. Robertson, A. Roodman, A. A. Salnikov, T. Schietinger, R. H. Schindler, J. Schwiening, A. Snyder,
A. Soha, S. M. Spanier, J. Stelzer, D. Su, M. K. Sullivan, H. A. Tanaka, J. Va'vra, S. R. Wagner,
M. Weaver, A. J. R. Weinstein, W. J. Wisniewski, D. H. Wright, C. C. Young

Stanford Linear Accelerator Center, Stanford, CA 94309, USA

P. R. Burchat, C. H. Cheng, T. I. Meyer, C. Roat

Stanford University, Stanford, CA 94305-4060, USA

R. Henderson

TRIUMF, Vancouver, BC, Canada V6T 2A3

W. Bugg, H. Cohn

University of Tennessee, Knoxville, TN 37996, USA

J. M. Izen, I. Kitayama, X. C. Lou

University of Texas at Dallas, Richardson, TX 75083, USA

F. Bianchi, M. Bona, D. Gamba

Università di Torino, Dipartimento di Fisica Sperimentale and INFN, I-10125 Torino, Italy

L. Bosisio, G. Della Ricca, S. Dittongo, L. Lanceri, P. Poropat, L. Vitale, G. Vuagnin

Università di Trieste, Dipartimento di Fisica and INFN, I-34127 Trieste, Italy

R. S. Panvini

Vanderbilt University, Nashville, TN 37235, USA

⁴ Also with University of California at San Diego, La Jolla, CA 92093, USA

C. M. Brown, P. D. Jackson, R. Kowalewski, J. M. Roney
University of Victoria, Victoria, BC, Canada V8W 3P6

H. R. Band, S. Dasu, M. Datta, A. M. Eichenbaum, H. Hu, J. R. Johnson, R. Liu, F. Di Lodovico, Y. Pan,
R. Prepost, I. J. Scott, S. J. Sekula, J. H. von Wimmersperg-Toeller, S. L. Wu, Z. Yu
University of Wisconsin, Madison, WI 53706, USA

T. M. B. Kordich, H. Neal
Yale University, New Haven, CT 06511, USA

1 Introduction

The technique of partial reconstruction of D^{*-} mesons (charge conjugate states are always implied), in which only the slow pion from $D^{*-} \rightarrow \bar{D}^0\pi^-$ is reconstructed, has been widely used in the past [1] to select large samples of reconstructed B mesons. This technique provides a way to measure the combination of the CKM unitarity triangle angles $(2\beta + \gamma)$ with $B^0 \rightarrow D^{*-}\pi^+$ decays [2]. The present measurement has been performed as a first step towards the goal of an analysis measuring the angle γ . In this respect, the reconstruction of the signal events, the rejection of the background, the characterization of the various background components and finally the study of the Δt resolution obtained in these events are important tools for a CP analysis. All these tools are presented here in the context of a B^0 lifetime measurement.

2 The *BABAR* detector and dataset

The data used in this analysis were collected with the *BABAR* detector at the PEP-II storage ring during 2000 and correspond to an integrated luminosity of 20.3 fb^{-1} collected at the $\Upsilon(4S)$ resonance and 2.6 fb^{-1} collected 40 MeV below the resonance for background studies (off-peak events).

PEP-II is an energy asymmetric storage ring, with positron and electron beam energies of about 3.11 and 9.0 GeV. The center-of-mass frame of the e^+e^- collision is therefore boosted along the z direction in the laboratory frame, enabling decay time-dependent measurements of B mesons through vertex reconstruction.

Samples of simulated $B\bar{B}$ and continuum events were analysed through the same analysis chain as the data. The equivalent luminosity of the generic simulated data is approximately equal to one third of the on-resonance data, while the equivalent luminosity of a specialized simulated sample containing $B^0 \rightarrow D^{*-}\pi^+$ decays followed by $D^{*-} \rightarrow \bar{D}^0\pi^-$ is 2.9 times larger than the on-resonance data sample.

A detailed description of the *BABAR* detector and the algorithms used for the track reconstruction, particle identification and selection of $B\bar{B}$ events is provided elsewhere [3]; a brief summary is given here.

Only charged particles are used for the partial reconstruction of the signal. Particles with momentum higher than 170 MeV/ c are reconstructed by matching hits in the silicon vertex tracker (SVT) with track elements in the drift chamber (DCH). Since tracks with momentum below 170 MeV/ c do not leave signals on many wires in the DCH due to the bending induced by the magnetic field, they are reconstructed in the SVT alone.

Electron and muon identification is used in veto mode for the selection of the fast pion. Electrons are identified on the basis of the energy deposited in the electromagnetic calorimeter (EMC), the track momentum and the energy loss in the DCH. Muons are selected by requiring deep penetration in the instrumented flux return (IFR).

The Cherenkov light emission measured in the particle identification detector (DIRC) is employed to reject kaons from the fast pion sample.

Neutral particles are reconstructed from clusters in the EMC that are unmatched to projected charged tracks. They are used only to compute event shape quantities.

3 The partial reconstruction technique

The $B^0 \rightarrow D^{*-}\pi^+$ decays are reconstructed using only the tracks from the π^+ (fast pion) and from the π^- (slow pion) in $D^{*-} \rightarrow \bar{D}^0\pi^-$. The fast pion momentum in the $\Upsilon(4S)$ rest frame is required to be in the range kinematically allowed for the decay $B^0 \rightarrow D^{*-}\pi^+$. For nominal values of the beam energies this momentum is in the range 2.114 - 2.404 GeV/ c . The momentum of the slow pion is required to be greater than 50 MeV/ c .

Assuming that the fast and slow pion come from the decay $B^0 \rightarrow D^{*-}\pi^+$ followed by the two body decay $D^{*-} \rightarrow X\pi^-$, it is possible to compute the mass of the recoiling system X averaged over an unmeasured angle due to the unknown direction of the B momentum in the $\Upsilon(4S)$ rest frame. For $B^0 \rightarrow D^{*-}\pi^+$ decays this recoil mass M_{rec} peaks at the D^0 mass with a width slightly less than 3 MeV/ c^2 . Assuming that the B momentum lies in the plane defined by the fast and slow pions momenta in the $\Upsilon(4S)$ rest frame, it is possible to compute the helicity angle of the pion in the D^{*-} rest frame as well as the candidate \bar{D}^0 direction.

Since the dominant source of background is continuum events, the selection procedure aims at reducing this contribution. The main requirements of this selection are the following:

- R2, the ratio of the second to the zeroth Fox-Wolfram moment [4], computed from charged particles, is required to be less than 0.35.
- No other tracks should be in a cone of opening angle 0.4 rad centered on the fast pion momentum in the $\Upsilon(4S)$ rest frame. This cut is effective against continuum events because in this case tracks tend to be clustered in jets.
- A Fisher discriminant F_D is computed from 15 event shape variables. Among these are the scalar sum of the momenta in the $\Upsilon(4S)$ rest frame of all tracks and neutrals, in nine 20° angular bins around the fast pion direction. The signal peaks at $F_D = -0.5$ while the continuum background peaks at $F_D = 0$. Events are required to satisfy $F_D < -0.1$.
- The cosine of the soft pion helicity angle is required to be larger than 0.4 in absolute value.

The B^0 decay point is determined from a vertex fit of the fast and slow pion tracks and the beam spot position in the plane perpendicular to the beam axis (the x - y plane). The beam spot is determined on a run-by-run basis using two-prong events [3]. Its size in the horizontal direction is 120 μm . Although the beam spot size in the y direction is only a few μm , a beam spot constraint of 30 μm is applied to account for the flight of the B^0 in the y direction. Only events for which the probability of the vertex fit is greater than 0.1% are considered further.

The decay point of the other B is determined from a subset of the remaining tracks in the event. All the tracks with a center-of-mass angle greater than 1 rad with respect to the candidate \bar{D}^0 direction are considered. This requirement is used to remove most of the tracks from the decay of the \bar{D}^0 daughter of the D^{*-} , which would otherwise bias the reconstruction of the other B vertex position. The selected tracks are then constrained to the beam spot in the x - y plane. The track with the largest contribution to the vertex χ^2 , if greater than 6, is removed and the fit iterated until no tracks fails this requirement. Vertices composed of just one track and the beam spot are rejected in order to reduce the number of poorly measured vertices. Simulation shows that after all these requirements in about 85% of signal events the other vertex has no tracks from the \bar{D}^0 decay.

Figure 1 shows the recoil mass distribution for on-resonance data events obtained by applying all the above cuts when the fast and slow pions have opposite-sign charges. These events are used to

measure the B^0 lifetime. Events with same-sign charges for the two pions are used as a background control sample (same-sign sample). Another background control sample is obtained by reversing the cut on the Fisher discriminant and requiring $F_D > 0$ ($B\bar{B}$ depleted sample).

The individual distributions shown in Figure 1 are obtained by fitting simultaneously to the on- and off-resonance data the contributions from

- $B^0 \rightarrow D^{*-}\pi^+$ events;
- $B^0 \rightarrow D^{*-}\rho^+$ events;
- $B^0 \rightarrow D^{*-}\ell^+\nu$ events;
- peaking $B\bar{B}$ background, where the fast and slow pions originate from the same B meson decay;
- non-peaking $B\bar{B}$ background, excluding the events from the previous four categories;
- peaking $c\bar{c}$ background, where the slow pion comes from the $D^{*-} \rightarrow \bar{D}^0\pi^-$ decay;
- continuum background excluding the events from the previous category.

All peaking backgrounds peak in the recoil mass distribution.

The shape of each contribution has been determined from the Monte Carlo simulation while all the normalizations have been left free in the fit except those for $B^0 \rightarrow D^{*-}\rho^+$ and $B^0 \rightarrow D^{*-}\ell^+\nu$ events which have been fixed to the value from the Monte Carlo simulation. The $B^0 \rightarrow D^{*-}\rho^+$ branching fraction is taken to be $(6.8 \pm 3.4) \cdot 10^{-3}$ [5] giving an estimate of 1570 events in the final sample from this decay mode. The fit gives 6971 ± 241 $B^0 \rightarrow D^{*-}\pi^+$ events. In the lifetime analysis to be described later, the $B^0 \rightarrow D^{*-}\rho^+$ events will be included as signal in addition to the 6971 $B^0 \rightarrow D^{*-}\pi^+$ events. Table 1 reports the composition of the selected sample for recoil mass larger than $1.86 \text{ GeV}/c^2$ (signal region sample) as determined by this fit.

Table 1: Composition of the data sample in the signal region.

Source	Fraction in Signal region (%)
$B^0 \rightarrow D^{*-}\pi^+$	46.1
$B^0 \rightarrow D^{*-}\rho^+$	9.3
$B^0 \rightarrow D^{*-}\ell^+\nu$	2.3
$B\bar{B}$ peaking	8.9
$B\bar{B}$ non peaking	11.5
uds	12.7
$c\bar{c}$ non peak.	5.2
$c\bar{c}$ peaking	4.0

4 The lifetime measurement

The PEP-II collider produces $B\bar{B}$ pairs moving along the beam direction (z axis) with an average Lorentz boost of $\langle\beta\gamma\rangle = 0.55$. The lifetime is determined by measuring the quantity $\Delta z = z_{decay} - z_{other}$, where z_{decay} (z_{other}) is the position along the beam line of the reconstructed $B^0 \rightarrow D^{*-}\pi^+$

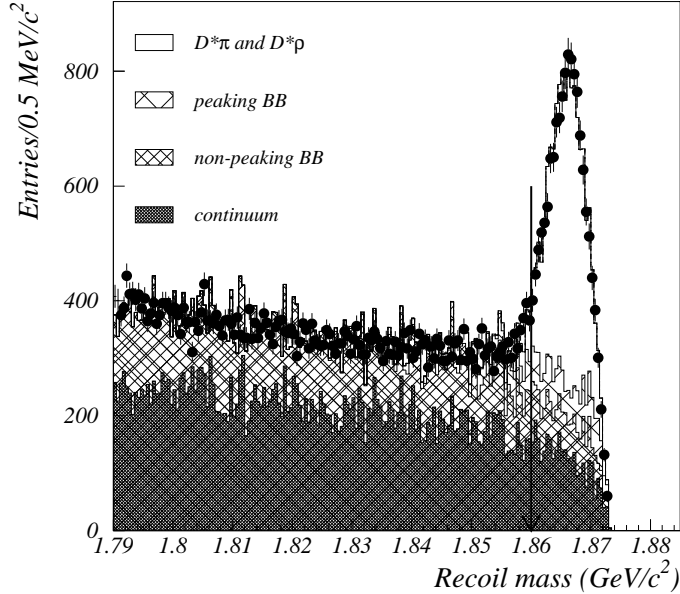


Figure 1: Recoil mass distribution obtained with the selection explained in the text when the fast and slow pion have opposite-sign charges. In this plot the small $B^0 \rightarrow D^{*-}\ell^+\nu$ component has been added to the peaking $B\bar{B}$ contribution. The continuum background includes the peaking $c\bar{c}$ component. The fit gives $6971 \pm 241 B^0 \rightarrow D^{*-}\pi^+$ events. The region to the right of the line corresponds to the signal region.

decay (other) vertex. To remove badly reconstructed vertices, all events for which $\sigma_{\Delta z} > 400\mu\text{m}$, where $\sigma_{\Delta z}$ is the uncertainty on Δz computed for each event, are rejected.

Residual tracks from the \bar{D}^0 decay, not removed by the track selection for the other B vertex, bias the reconstruction of the other B vertex position. This bias is removed by correcting the Δz value for each event with a correction function determined from the simulated signal sample as a function of Δz .

The proper time difference between B decays is then computed with the relation $\Delta t = \Delta z / \langle c\beta\gamma \rangle$. A fit with a double Gaussian to the Δt residuals in the Monte Carlo simulation shows that 75% of the events are contained in the narrower Gaussian, which has a width of 0.8 ps.

The lifetime τ_{B^0} is obtained from an unbinned maximum likelihood fit to the two-dimensional Δt , $\sigma_{\Delta t}$ distribution. The Δt distribution of signal events is described by the convolution of the decay probability distribution

$$f(\Delta t_{true} | \tau_{B^0}) = \frac{1}{2\tau_{B^0}} e^{-|\Delta t_{true}|/\tau_{B^0}}, \quad (1)$$

with the experimental resolution function, which is represented by the sum of three Gaussian

distributions. The first two, accounting for more than 99% of the events, have the form

$$G(\delta(\Delta t), \sigma_{\Delta t}) = \frac{1}{\sqrt{2\pi}S\sigma_{\Delta t}} e^{-\frac{(\delta(\Delta t) - b\sigma_{\Delta t})^2}{2S^2\sigma_{\Delta t}^2}} \quad (2)$$

where $\delta(\Delta t) = \Delta t - \Delta t_{true}$ is the difference between the measured and the true value of Δt , b is a bias due to the charm tracks in the other vertex and the scale factor S is introduced to account for possible misestimation of the error on the proper time difference Δt . The third Gaussian of fixed bias $b = 0$ and scale factor $S = 6$ is added to account for badly mismeasured events (“outliers”).

The $B^0 \rightarrow D^{*-}\rho^+$ resolution function has been found with Monte Carlo simulation to be the same as for signal events. In the fit for the B^0 lifetime the $B^0 \rightarrow D^{*-}\rho^+$ events are considered as signal events. Events coming from the decay $B^0 \rightarrow D^{*-}\ell^+\nu$ are added to the $B\bar{B}$ peaking component and the Δt distribution of the latter is assumed to be equal to the $B\bar{B}$ non-peaking component.

The Δt distribution of the B background contribution is described by a resolution function similar to that used for the signal. In this case the lifetime parameter represents an effective B lifetime which has been fitted independently from the signal lifetime.

The Δt distribution for uds events is described by the sum of three Gaussians while the Δt distribution for $c\bar{c}$ events has been described by the sum of a Gaussian plus the same Gaussian convoluted with an exponential term to account for the effective charm hadron lifetime.

The function used to fit the data is the weighted sum of four contributions:

$$F(\Delta t, \sigma, \tau_{B^0}) = [1 - f_{B\bar{B}}(M_{rec}) - f_{uds}(M_{rec}) - f_{c\bar{c}}(M_{rec})]F_{B^0}(\Delta t, \sigma, \tau_{B^0}) + f_{B\bar{B}}(M_{rec})F_{B\bar{B}}(\Delta t, \sigma) + f_{uds}(M_{rec})F_{uds}(\Delta t, \sigma) + f_{c\bar{c}}F_{c\bar{c}}(\Delta t, \sigma)$$

where the functions F_{B^0} , $F_{B\bar{B}}$, F_{uds} and $F_{c\bar{c}}$ describe the measured decay time difference distributions for the signal, $B\bar{B}$ background, uds and $c\bar{c}$ events, respectively. $f_{B\bar{B}}$, f_{uds} and $f_{c\bar{c}}$ are the probabilities that the event is from the $B\bar{B}$, uds and $c\bar{c}$ background, computed for each event on the basis of the measured value of the recoil mass M_{rec} .

The key parameters describing the Δt distributions for the background events are fitted on the $B\bar{B}$ depleted control sample for the continuum background and on the same-sign sample for the $B\bar{B}$ background. The $B\bar{B}$ depleted control sample has been used because the integrated luminosity of the off resonance sample is not sufficient to precisely determine the parameters of the continuum background. An alternative parameterization obtained by fitting the side-band control sample has also been tried giving compatible results.

All the parameters describing the signal resolution function are free in the fit except the bias of the second Gaussian which is fixed to the value found on the signal Monte Carlo sample.

The result of the fit to the signal region sample in the range $|\Delta t| < 15$ ps is $\tau_{B^0}^{raw} = 1.524 \pm 0.040$ ps, where the error is statistical only. Figure 2 shows the comparison between the measured Δt distribution and the fit result. All the fitted parameters appear in Table 2.

The raw value $\tau_{B^0}^{raw}$ value is corrected for a small bias, 0.014 ± 0.020 ps, observed when fitting the signal Monte Carlo sample using the same procedure, yielding the corrected value $\tau_{B^0} = 1.510 \pm 0.040$ ps.

5 Systematic uncertainties and cross-checks

The systematic error on τ_{B^0} is computed by adding in quadrature the contribution from several sources, described below and summarised in Table 3.

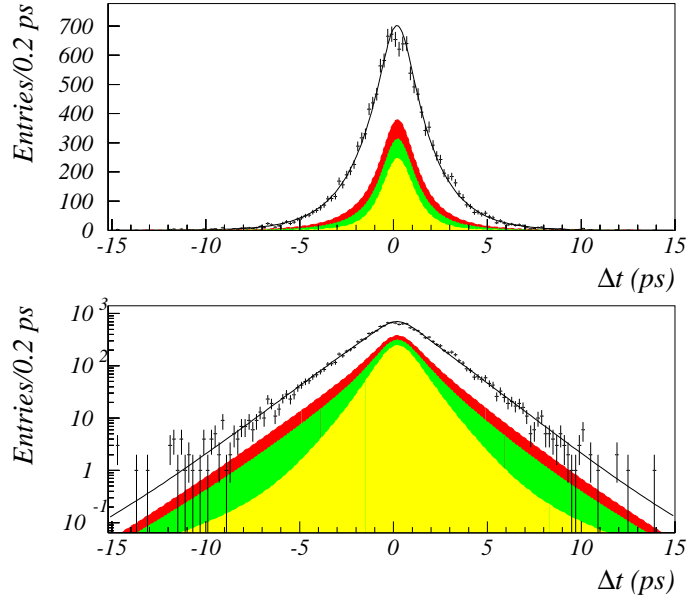


Figure 2: Decay time difference (Δt) distribution for the signal region sample on a linear (upper) and logarithmic (lower) scale. The curve shows the result of the unbinned maximum likelihood fit. The shaded areas represent from bottom to top the following contributions in the fit: $uds+c\bar{c}$, non-peaking $B\bar{B}$, peaking $B\bar{B}$ and signal.

The fractions of the various background components are varied by their uncertainties obtained from the recoil mass fit. The parameters of the various background Δt distributions are also varied by their uncertainties, properly accounting for their mutual correlations. The effective lifetime of the $B\bar{B}$ peaking component is varied by ± 0.044 ps corresponding to the difference between the value found in the data and in the Monte Carlo sample. An alternate resolution function for this component has also been tried with negligible variation on τ_{B^0} .

The bias of the wide Gaussian, the only parameter of the signal resolution function which is not fitted, is varied in a conservative range. Several different analytical expressions are used to represent the small fraction of outliers. The fit range is varied from $(-10, 10)$ ps to $(-20, 20)$ ps. The parameters of the Δz correction are varied according to the uncertainty due to the finite signal Monte Carlo sample size. The systematic uncertainty related to this correction is estimated from the effect of a $\pm 5\%$ variation on the fraction of fitted other- B vertices which have no tracks from the \bar{D}^0 decay.

The z length scale is determined to about 0.4% from secondary interactions with a beam pipe section of known length. The statistical uncertainty of the residual bias found on signal Monte Carlo events is also added to the systematic error.

The total systematic error of ± 0.038 ps is found by adding in quadrature the uncertainties from the above sources.

Table 2: Result of the fit to the data. The uds and $c\bar{c}$ backgrounds have been fitted on the $B\bar{B}$ depleted control sample. The $B\bar{B}$ background has been fitted on the same-charge control sample.

Parameter description	Value
uds narrow Gaussian fraction	0.972 ± 0.079
uds narrow Gaussian bias	0.181 ± 0.020
uds narrow Gaussian scale	1.194 ± 0.037
uds outliers fraction	0.0070 ± 0.0028
$c\bar{c}$ narrow Gaussian bias	0.342 ± 0.039
$c\bar{c}$ narrow Gaussian scale	1.404 ± 0.091
$c\bar{c}$ lifetime fraction	0.296 ± 0.102
$c\bar{c}$ lifetime	0.784 ± 0.196 ps
$B\bar{B}$ lifetime	1.611 ± 0.044 ps
$B\bar{B}$ narrow Gaussian fraction	0.721 ± 0.104
$B\bar{B}$ narrow Gaussian bias	0.326 ± 0.131
$B\bar{B}$ narrow Gaussian scale	0.863 ± 0.210
$B\bar{B}$ outliers fraction	0.000 ± 0.013
raw B^0 lifetime	1.524 ± 0.040 ps
signal narrow Gaussian fraction	0.962 ± 0.065
signal narrow Gaussian bias	0.140 ± 0.058
signal narrow Gaussian scale	1.336 ± 0.082
signal wide Gaussian bias	-0.5 (Fixed)
signal wide Gaussian scale	2.640 ± 1.420
signal outliers fraction	0.0049 ± 0.0078

The dependence of the result on several different variables (angular width of the cone used to reject the \bar{D}^0 tracks, fast pion momentum, polar and azimuthal angles) has been studied: no statistically significant effect is found.

6 Conclusion

In conclusion the neutral B meson lifetime has been measured with a sample of 6971 ± 241 partially reconstructed $B^0 \rightarrow D^{*-} \pi^+$ decays:

$$\tau_0 = 1.510 \pm 0.040 \pm 0.038 \text{ ps.}$$

This preliminary value is consistent with other recent *BABAR* measurements [6] and with the world average B^0 lifetime [5].

7 Acknowledgments

We are grateful for the extraordinary contributions of our PEP-II colleagues in achieving the excellent luminosity and machine conditions that have made this work possible. The success of this project also relies critically on the expertise and dedication of the computing organizations that support *BABAR*. The collaborating institutions wish to thank SLAC for its support and the kind hospitality extended to them. This work is supported by the US Department of Energy and National

Table 3: Summary of contributions to the systematic error.

Source	Error (fs)
Background Parameters	13
Fractional composition	20
Δz correction (MC)	6
Δz correction (model)	17
Bias of the wide Gaussian (signal)	6
Outliers	9
Δt range	9
MC bias	20
z scale	6
Total	38

Science Foundation, the Natural Sciences and Engineering Research Council (Canada), Institute of High Energy Physics (China), the Commissariat à l’Energie Atomique and Institut National de Physique Nucléaire et de Physique des Particules (France), the Bundesministerium für Bildung und Forschung (Germany), the Istituto Nazionale di Fisica Nucleare (Italy), the Research Council of Norway, the Ministry of Science and Technology of the Russian Federation, and the Particle Physics and Astronomy Research Council (United Kingdom). Individuals have received support from the A. P. Sloan Foundation, the Research Corporation, and the Alexander von Humboldt Foundation.

References

- [1] ARGUS Collaboration, H. Albrecht et al., Phys. Lett. B **324**, 249 (1994); CLEO Collaboration, J. Bartelt et al., Phys. Rev. Lett. **71**, 1680 (1993).
- [2] The *BABAR* Collaboration, P. F. Harrison and H. R. Quinn, ed., The *BABAR* Physics Book, SLAC-R-504 (1998).
- [3] The *BABAR* Collaboration, B. Aubert et al., Nucl. Instr. and Methods A **479**, 1 (2002).
- [4] G.C. Fox and S. Wolfram, Phys. Rev. Lett. **41**, 1581 (1978).
- [5] D.E. Groom et al., Review of Particle Physics, Eur. Phys. Jour. C **15**, 1 (2000).
- [6] The *BABAR* Collaboration, B. Aubert et al., Phys. Rev. Lett. **87**, 201803 (2001); The *BABAR* Collaboration, B. Aubert et al., SLAC-PUB-9128, hep-ex/0202005, to be published in Phys. Rev. Lett.